

THE PROFILED CYLINDRICAL SLIDEWAY
Load capacity and design

by

Lars Holmdahl

This is an updated version of the original report from May 1985. The original work was done two years prior to publication, as described in the report. In this 2nd edition typos have been corrected, the layout has been modernized, some plotted curves have been added to the original, and mathematical expressions have been expanded and rewritten using Mathcad.

Today, some 32 years later, it is easy to forget the conditions under which we worked then. The report was written on an IBM typewriter (do you remember Tip-Ex?) with interchangeable balls (for changing typeface). Computing, if you could afford it and had an account at the University computer center, was done on mainframe computers (IBM 360). You paid for cpu-time. Jobs were batched. No graphical interface. Input was 80 positions per line, etc. The School of Machine Design and Naval Architecture had just acquired a mini computer from Norsk Data. That came in handy for writing the formulas.

The numerical calculations in the original report were done on a Texas Instruments Ti59 programmable calculator. The closed form analytical solution was found after a week's daily work with pen and paper by aid of, always dependable, Gradshteyn and Ryzhik: Table of Integrals, Series, and Products.

Göteborg May 2015

Lars Holmdahl, Dr.-Ing.

Report number: 1985.05.15
Division of machine elements
Chalmers University of Technology
Göteborg Sweden

ABSTRACT

Only one solution to the load capacity problem of a profiled cylindrical slideway is given in the literature; that of Prof. Dr.-Ing. H. Brendel. Unfortunately the one-dimensional analytical solution given by Prof. Brendel is erroneous due to a mathematical error in his first equation.

The correct solution is given in this report. The closed form solution is compared with both a one-dimensional numerical solution and a two-dimensional finite-difference solution. The agreement is good.

Oil consumption, temperature rise and friction are briefly discussed. Design rules based on actual engineering experience are given.

FOREWORD

In the summer of 1983 I received a telephone call from the manager of a factory producing wood working machines. They had recently designed and started production of slider crank type briquette machines and now the first two machines had failed through galling in the slider bearing after less than 200 hours of service time.

The machines of the competitors were basically of the same design. The slideways were boundary lubricated and wore out in about 1000 hours.

Obviously the design would be greatly improved if the bearing could be made to operate in the hydrodynamic regime - but how?

A brief search in the literature was of no help so a first crude theory was compiled. In parallel to this a thorough literature search was undertaken during which the theory of Prof. Brendel was found. A close examination revealed that his theory was erroneous. Brendel had erred in his first equation. Therefore the present theory was compiled.

In the fall of 1984 when the first two modified machines surpassed 10 000 hours of service time, it was felt that the profiled cylindrical slideway had proved to be such a great asset to the design engineer that this report should be written.

Göteborg May 1985

Lars Holmdahl

CONTENTS

Notation	2
Introduction	3
Load capacity:	
one conical section, parallel axis.....	4
tilting	9
the influence of the cylindrical section (parallel axis)	14
Circumferential flow	15
Optimizing	16
Oil consumption, temperature rise and friction	17
The influence of oil grooves.....	19
Design rules	20
References	21
Diagrams	22

NOTATION

D	bushing ID
d	slider, largest diameter
L	length of one profiled section
cL	length of one cylindrical section
t	profile depth (half the difference between the sliders largest and smallest diameter)
$r=d/2$	radius
v	sliding velocity
	dynamic viscosity
$\psi := \frac{D-d}{d}$	bearing clearance (nondimensional)
e	slider radial displacement (eccentricity)
$\varepsilon := \frac{2 \cdot e}{\psi \cdot d}$	relative eccentricity
$\kappa := \frac{2 \cdot t}{\psi \cdot d}$	profile parameter (nondimensional)
	circumferential angle
$h_0 := \frac{\psi \cdot d}{2} \cdot (1 - \varepsilon \cdot \cos(\theta))$	minimum film thickness at the rear end
W_0	load capacity of one profiled section (nondimensional)
$W := \eta \cdot v \cdot d \cdot \left(\frac{L}{\psi \cdot d} \right)^2 \cdot W_0$	load capacity of one profiled section

INTRODUCTION

Up until now slideways have been made to operate within the boundary lubrication regime. By giving the mating surfaces a slight waviness it has been possible to achieve mixed lubrication. Mixed and boundary lubricated bearings wear out fairly fast. The maximum nominal pressure is lower and the friction higher than in a hydrodynamic bearing. The boundary lubricated bearing is also sensitive to contaminations in the oil e.g. dust and wear particles.

In order to avoid the drawbacks of traditional slideways one can use new machine elements such as roller bushings or make hydrodynamic slideways.

Hydrodynamic slideways have been sparsely treated in the literature and almost only in the last decade. The first article was published in 1952 (1). Maybe it is this lack of literature and design rules that is especially responsible for the hydrodynamic slideway not being used in spite of its advantages:

- a) high bearing stiffness (1),(2).
- b) low production cost
- c) easy to employ (no adjustments or fine tuning)
- d) tolerates high nominal pressure
- e) very low wear
- f) very high transient capacity due to squeeze-effect

This report intends to give a simple theory for the load capacity of the hydrodynamic cylindrical slideway when the slider is parallel to the bushing and when it is inclined/tilted a small angle.

LOAD CAPACITY

One conical section, parallel axis

A slider moves in a bushing, figure 1. When there is no load on the slider, it is coaxial to the bushing. Now apply a load W on the slider, figure 2, this moves the slider radially downwards until the now unsymmetrical pressure distribution balances the force W .

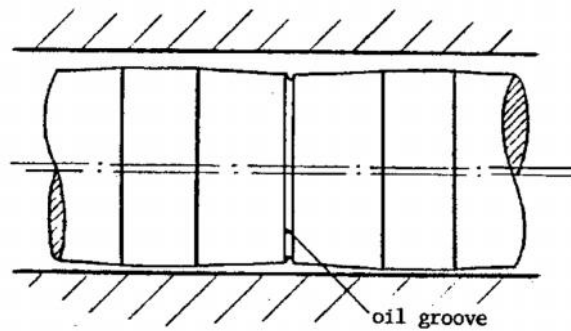


Figure 1. A profiled cylindrical slider in a bushing

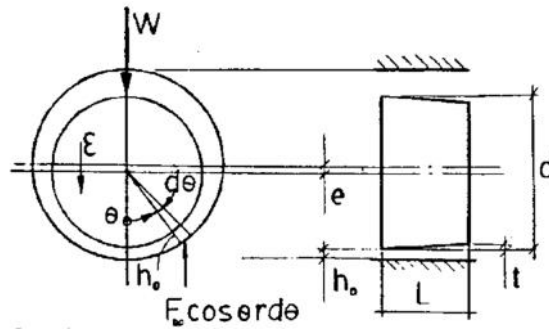


Figure 2. Load and load reaction on one conical section

If we ignore any circumferential oil flow, that is: if the oil flows in a straight line through the bearing, its load capacity can be calculated using the theory for a plane pad bearing of infinite width. For a pad bearing of infinite width the load capacity per unit width is (3):

$$F_0 := 6 \cdot \eta \cdot v \cdot \left(\frac{L}{h_0} \right)^2 \cdot \delta^2 \cdot \left(\ln \left(\frac{1 + \delta}{\delta} \right) - \frac{2}{1 + 2\delta} \right)$$

With

$$\delta = \frac{h_0}{t} = \frac{\psi \cdot r}{t} (1 - \varepsilon \cos \theta) = \frac{\psi \cdot d}{2t} (1 - \varepsilon \cos(\theta)) = \frac{1}{\kappa} (1 - \varepsilon \cos(\theta))$$

We can rewrite the expression for F_0

$$F_0 := \eta \cdot v \cdot \left(\frac{L}{\psi \cdot d} \right)^2 \cdot \frac{24}{\kappa^2} \cdot \left[\ln \left(1 + \frac{\kappa}{1 - \varepsilon \cdot \cos(\theta)} \right) - \frac{2}{1 + \frac{2}{\kappa} \cdot (1 - \varepsilon \cdot \cos(\theta))} \right]$$

Integrating around the circumference, figure 2, we get the load capacity W of one

profiled section:

$$W := 2 \cdot \int_0^{\pi} \mathbf{F}_0 \cdot \frac{d}{2} \cdot \cos(\theta) d\theta$$

$$W := \eta \cdot v \cdot d \cdot \left(\frac{L}{\psi \cdot d} \right)^2 \cdot \int_0^{\pi} \frac{24}{\kappa^2} \cdot \left[\ln \left(1 + \frac{\kappa}{1 - \varepsilon \cdot \cos(\theta)} \right) - \frac{2}{1 + \frac{2}{\kappa} \cdot (1 - \varepsilon \cdot \cos(\theta))} \right] \cdot \cos(\theta) d\theta$$

This can be written

$$W := \eta \cdot v \cdot d \cdot \left(\frac{L}{\psi \cdot d} \right)^2 \cdot W_0(\varepsilon, \kappa)$$

$$W_{0n}(\varepsilon, \kappa) := \frac{24}{\kappa^2} \cdot \int_0^{\pi} \left[\ln \left(1 + \frac{\kappa}{1 - \varepsilon \cdot \cos(\theta)} \right) - \frac{2}{1 + \frac{2}{\kappa} \cdot (1 - \varepsilon \cdot \cos(\theta))} \right] \cdot \cos(\theta) d\theta$$

Numerical solutions of W_{0n} for different non dimensional profile parameters κ are plotted as functions of relative eccentricity ε in figure 3, below.

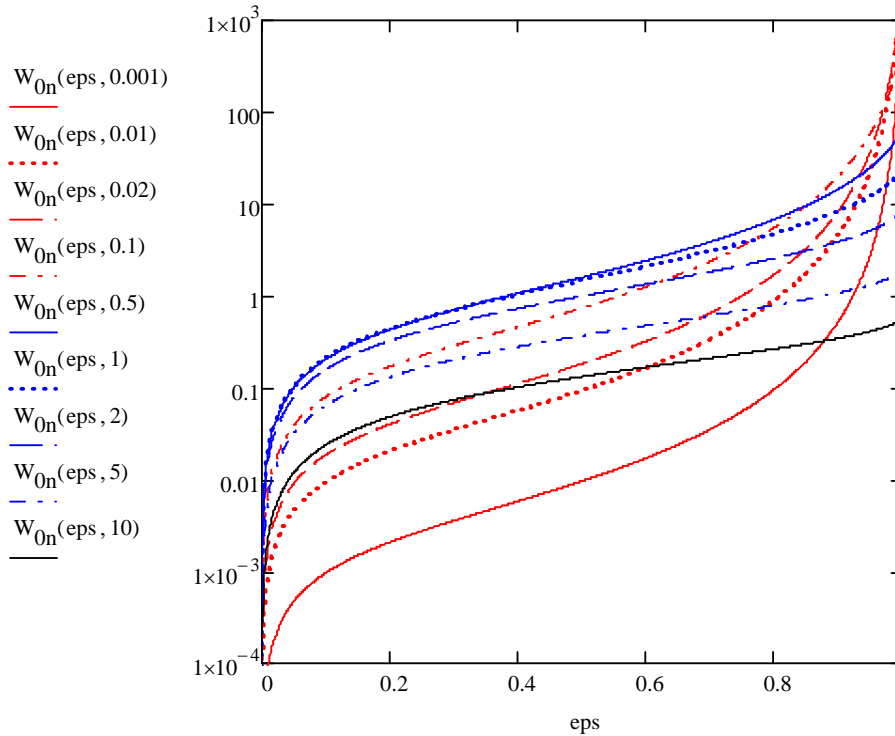


Figure 3. Numerical solutions of W_0 for different non dimensional profile parameters κ are plotted as functions of relative eccentricity ε

There is an analytical closed form solution to W_0 that gives identical solutions to the numerical solution.

$$W_0(\varepsilon, \kappa) := \frac{24\pi}{\kappa^2 \cdot \varepsilon} \left[\sqrt{(1 + \kappa)^2 - \varepsilon^2} - \sqrt{1 - \varepsilon^2} - \frac{\kappa}{\sqrt{1 - \left(\frac{2 \cdot \varepsilon}{2 + \kappa}\right)^2}} \right]$$

The last part of the solution is the same as the second part of the solution given in ref (4). The first part is not.

It is informative to view W_0 as a function of κ for different ε , figure 4.

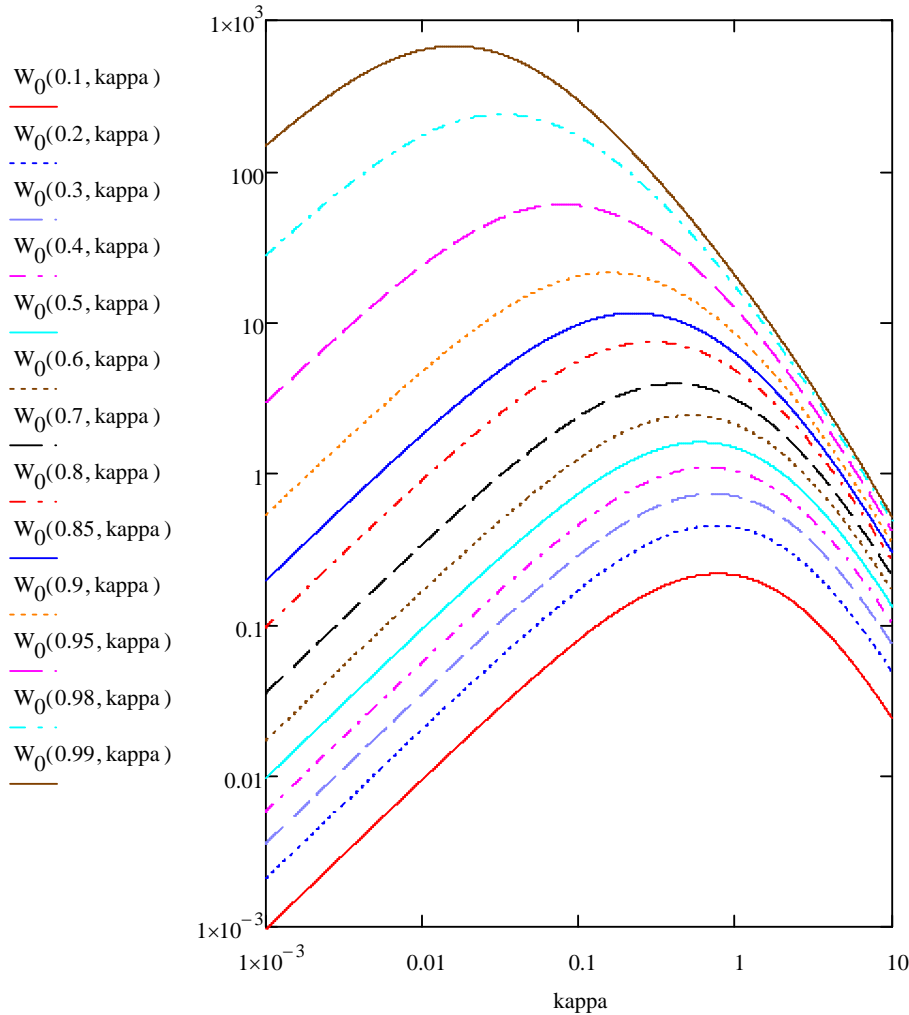


Figure 4. The nondimensional load capacity W_0 increases with relative eccentricity ε

It is evident from the curves that, from a load capacity perspective, for every κ there is an optimal ε . Furthermore κ should always be less than one. This leaves us with a rather narrow band of alternatives. Figure 5 gives a closer view.

The original set of curves (from the original 1985 version of this report) showing the dimensionless load capacity W_0 as a function of the nondimensional profile parameter κ and the relative eccentricity ε is shown in diagrams 1 and 2 at the end of the report.

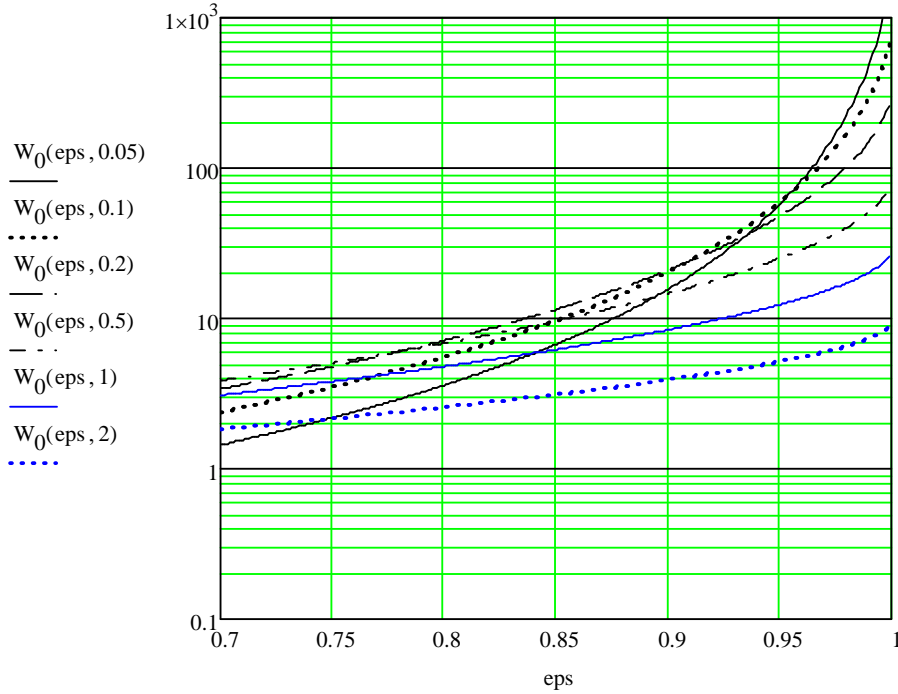


Figure 5. A closer look of W_0 for different non dimensional profile parameters κ as functions of relative eccentricity ϵ

Finding optimum κ and ϵ

For a plane pad bearing we have maximum load capacity for

$$\frac{t}{h_0} + 1 = 2.2$$

Which in our case becomes

$$\frac{t}{h_0} = \frac{2t}{\psi \cdot d(1 - \epsilon \cos(\theta))} = \frac{\kappa}{1 - \epsilon \cos(\theta)} = 1.2$$

This hints at a possible connection between optimum parameters that looks like this

$$\kappa = z(1 - \epsilon)$$

If we plot the nondimensional load capacity W_0 for $0.6 < \epsilon < 0.95$ and $0 < z < 6$, we see that there is an optimum range of $1 < z < 1.8$, figure 6. This gives us optimum profile parameter as a function of relative eccentricity, figure 7.

$$1 - \epsilon < \kappa < 1.8(1 - \epsilon)$$

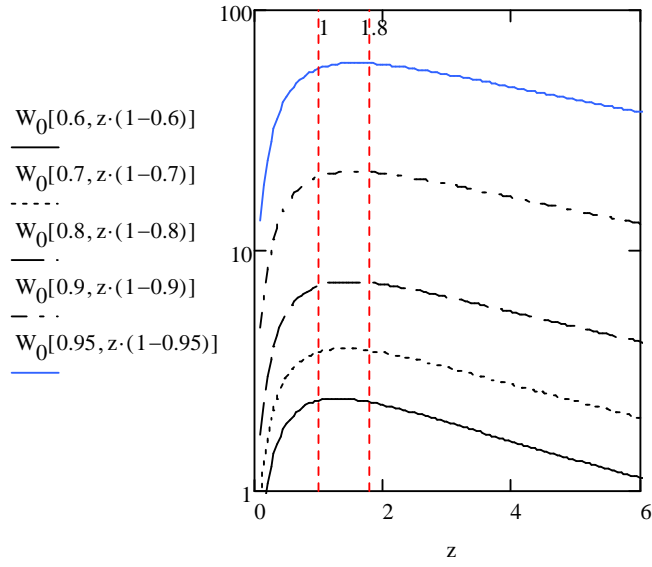


Figure 6. Optimum range z is 1-1.8

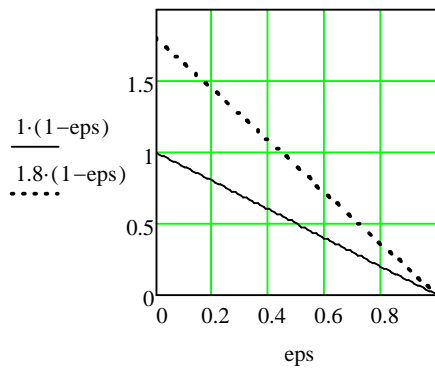


Figure 7. Optimum profile parameter κ as a function of relative eccentricity ϵ

Tilting

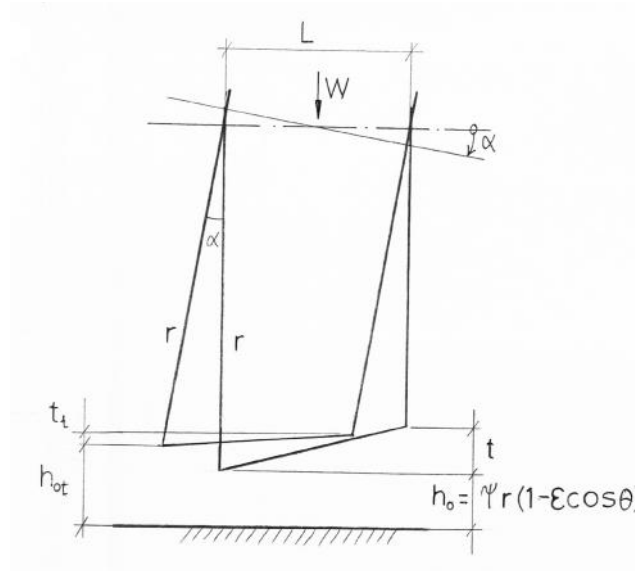


Figure 8. A tilted conical section

In practical applications the slider will often be tilted. The geometry for this case is given in figure 8. The leading and trailing corners are moved $r\alpha$ and $L\alpha/2$. The conditions after tilting an angle α is given subscript t. We have

$$h_{0t} := h_0 - \frac{L\alpha}{2} \cdot \cos(\alpha) \cdot \cos(\theta) + r \cdot \alpha \cdot \sin(\alpha) \cdot \cos(\theta)$$

$$t_t := t + \left(\frac{-L\alpha}{2} \cdot \cos(\alpha) - r \cdot \alpha \cdot \sin(\alpha) - \frac{L\alpha}{2} \cdot \cos(\alpha) + r \cdot \alpha \cdot \sin(\alpha) \right) \cdot \cos(\theta)$$

Using that α is a small angle and neglecting α^2 we get

$$h_{0t} := h_0 + \frac{L\alpha}{2} \cdot \cos(\theta)$$

$$t_t := t - L\alpha \cdot \cos(\theta)$$

An interesting question is how much the slider can tilt. If we have one conical section only (no cylindrical section), then max tilt is

$$\alpha = \pm t/L$$

If however, the slider inside the bushing is of length $n \cdot d$, where typically $n \approx 2$ or larger, while L is a fraction of d , say $d/L \approx 10$, and $0.002 < \psi < 0.01$, say $\psi = 0.004$, then we get a much lower value

$$\alpha = \psi d / nd = \psi / n = 0.004 / 2 = 0.002 \text{ [radians]}$$

The possible tilt is thus very small. For the remainder we assume that $L\alpha$ is a fraction of profile depth t , so that

$$L\alpha = \xi t$$

Film thickness at the trailing edge and profile depth at tilt can now be written

$$h_{0t} := t \cdot \left[\frac{1}{\kappa} \cdot (1 - \varepsilon \cdot \cos(\theta)) + \frac{\xi}{2} \cdot \cos(\theta) \right]$$

$$t_t := t \cdot (1 - \xi \cdot \cos(\theta))$$

A small rewriting of the force F_{0t} of the tilted case yields

$$F_{0t} := 6 \cdot \eta \cdot v \cdot \left(\frac{L}{\psi \cdot d} \right)^2 \cdot \frac{4}{\kappa^2 \cdot (1 - \xi \cdot \cos(\theta))^2} \cdot \left(\ln \left(1 + \frac{t_t}{h_{0t}} \right) - \frac{2}{1 + 2 \cdot \frac{h_{0t}}{t_t}} \right)$$

The load capacity is, as before

$$W_t := d \cdot \int_0^\pi F_{0t} \cdot \cos(\theta) \, d\theta$$

$$W_t := \eta \cdot v \cdot d \cdot \left(\frac{L}{\psi \cdot d} \right)^2 \cdot \int_0^\pi \frac{24}{\kappa^2 \cdot (1 - \xi \cdot \cos(\theta))^2} \cdot \left(\ln \left(1 + \frac{t_t}{h_{0t}} \right) - \frac{2}{1 + 2 \cdot \frac{h_{0t}}{t_t}} \right) \cdot \cos(\theta) \, d\theta$$

Which as before becomes

$$W_t := \eta \cdot v \cdot d \cdot \left(\frac{L}{\psi \cdot d} \right)^2 \cdot W_{0t}(\varepsilon, \kappa, \xi)$$

$$W_{0t}(\varepsilon, \kappa, \xi) := \int_0^\pi \frac{24}{\kappa^2 \cdot (1 - \xi \cdot \cos(\theta))^2} \cdot \left(\ln \left(1 + \frac{t_t}{h_{0t}} \right) - \frac{2}{1 + 2 \cdot \frac{h_{0t}}{t_t}} \right) \cdot \cos(\theta) \, d\theta$$

It is beyond the capacity of this author to find a closed form solution to this integral. A numerical solution can be found by expanding the expressions for profile depth and trailing edge film thickness, yielding

$$W_{0t}(\varepsilon, \kappa, \xi) := \int_0^\pi \frac{24}{\kappa^2 \cdot (1 - \xi \cdot \cos(\theta))^2} \cdot \left[\ln \left[1 + \frac{1 - \xi \cdot \cos(\theta)}{\left[\frac{1}{\kappa} \cdot (1 - \varepsilon \cdot \cos(\theta)) + \frac{\xi}{2} \cdot \cos(\theta) \right]} \right] - \frac{2}{1 + \frac{\frac{2}{\kappa} \cdot (1 - \varepsilon \cdot \cos(\theta)) + \xi \cdot \cos(\theta)}{1 - \xi \cdot \cos(\theta)}} \right] \cdot \cos(\theta) \, d\theta$$

Visual inspection shows that by putting $\xi = 0$ the expression reduces to W_0 , the case without tilt.

In order to compare with previous results we create the quotient tilted and non-tilted slider.

$$Q_0(\varepsilon, \kappa, \xi) := \frac{W_{0t}(\varepsilon, \kappa, \xi)}{W_0(\varepsilon, \kappa)}$$

Interesting parameter ranges are

$$0.8 < \varepsilon < 1$$

$$0.05 < \kappa < 1$$

$$-0.5 < \xi < 1$$

Plotting Q_0 as a function of tilt parameter ξ for relative eccentricities $\varepsilon = 0.8$ and different profile depth parameters κ , we see that tilting the slider reduces load carrying capacity if the tilt angle $\alpha > 0$, and may increase load capacity if $\alpha < 0$, figure 9.

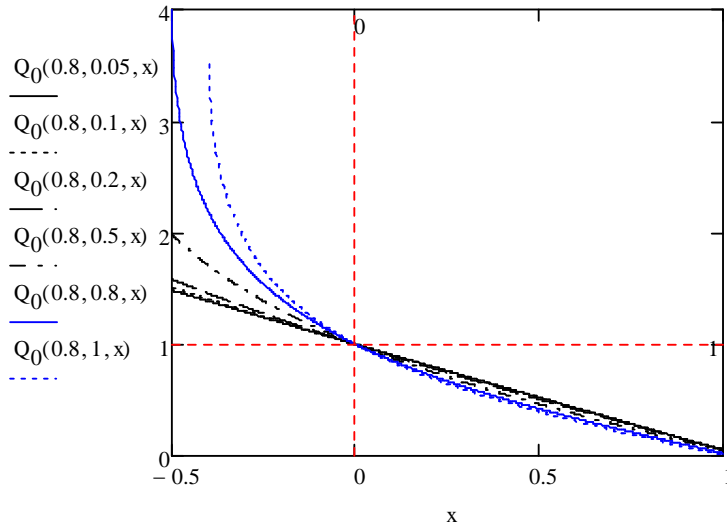


Figure 9. W_{0t} for tilted slider divided by W_0 for non-tilted slider. Tilt parameter $x = \xi$

A reduction of load capacity due to tilt, may be compensated by a slight increase in eccentricity.

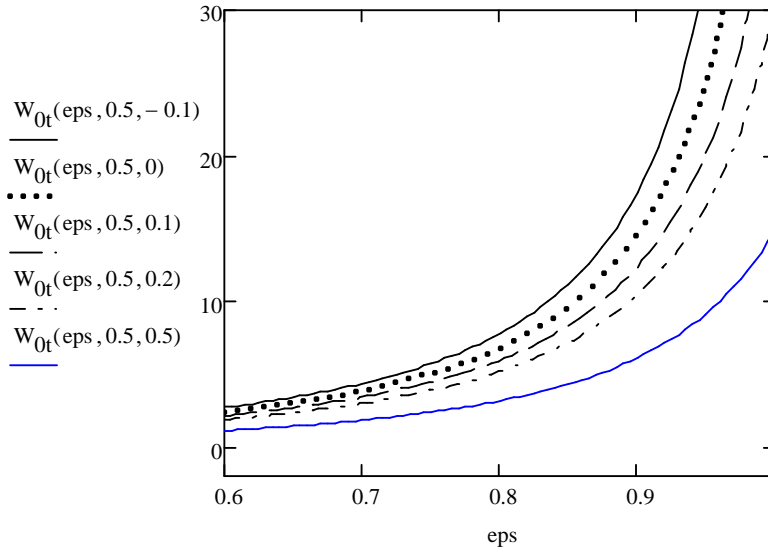


Figure 10. Nondimensional load capacity as a function of relative eccentricity ϵ for $\kappa = 0.5$ and different tilt

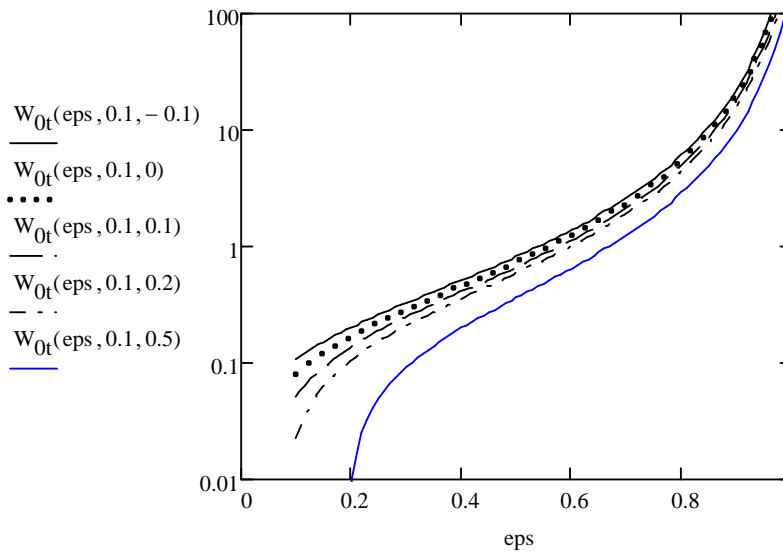


Figure 11. Nondimensional load capacity as a function of relative eccentricity ϵ for $\kappa = 0.1$ and different tilt

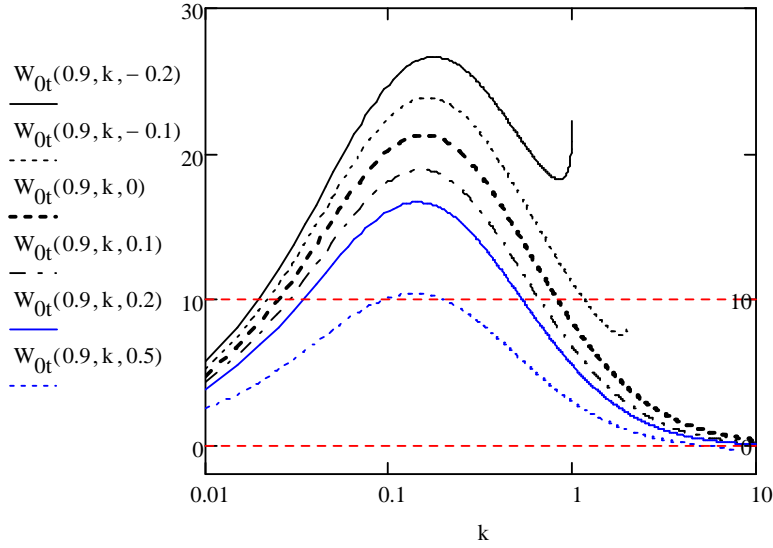


Figure 12. Nondimensional load capacity as a function of nondimensional profile depth. Relative eccentricity 0.9. Zero tilt is fat black dotted line.

Originally, in this report, dimensionless load capacity W was calculated for different degrees of tilt; $\alpha L/t$ and shown as an addendum to the report in diagrams 3 through 9. These plots have been removed from this, the 2nd edition of the report. They do not give much useful information and besides, if needed, the formulas given can be immediately used for example in Mathcad.

The influence of the cylindrical section (parallel axis)

In the analysis above, the pressure at the end of the conical section was assumed to be zero. In practice however the conical section is followed by a cylindrical one. This means that, as long as the slider and bushing are parallel, the pressure is not zero at the end of the conical section but falls gradually as the oil flows along the cylindrical section.

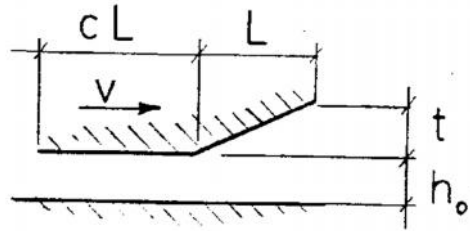


Figure 13. Conical section followed by a cylindrical section

The load capacity for this case is not evaluated. However, we can note that a pad bearing that consists of a tapered part followed by a flat part, a so-called tapered-land pad bearing, of equal length to a tapered pad bearing has somewhat (+16%) higher load capacity at the optimum proportions of $c = 0.2$ (figure 13). For c close to this value, the tapered-land bearing has about the same load capacity as a tapered pad bearing of equal length.

Cylindrical areas are useful for providing landing and starting zones dominated by boundary lubrication and for providing squeeze effect for handling dynamic loads.

CIRCUMFERENTIAL FLOW

In reality there is of course a circumferential flow from the high pressure side of the bearing towards the low pressure side. This flow was neglected in the formulas above. In order to get an estimate of the error introduced by neglecting the side flow, the Reynolds equation:

$$\frac{\partial}{\partial x} \left(h^3 \frac{\partial p}{\partial x} \right) + \frac{\partial}{\partial z} \left(h^3 \frac{\partial p}{\partial z} \right) = 6\eta v \frac{\partial p}{\partial x}$$

was solved with a finite difference method using a 19*61 mesh. With the pressure p known, the load capacity W was calculated according to:

$$W = 2 \int_0^\pi \int_0^L p(x, \theta) \cos \theta \, d \, dx d\theta$$

In this case the pressure distribution depends also upon the relation between the length of the profiled section and the slider diameter. Therefore a new dimensionless group that does not contain the length L is used:

$$W = \frac{\eta v d}{\psi^2} W_1(\beta, \kappa, \varepsilon)$$

The non-dimensional load capacity W_1 is shown in diagrams 10 through 18 in the addendum.

At eccentricity $\varepsilon = 0$, there is no circumferential pressure gradient and thus no side flow. As ε grows, so do the pressure gradient and the side flow. The 2-dim solution therefore always gives a smaller value than the 1-dim solution.

A comparison of 1-dim to 2-dim solution shows that for short sections, equal to or smaller than $0.1d$ there is virtually no difference between the two solutions, indicating that side flow is negligible at small L/d . Even for $L/d = 0.3$ (and $0.2 < \kappa < 5$) the difference is of little practical importance since a small increase in eccentricity compensates for the difference in load capacity.

It is at large ε and small κ that the difference is at its largest. Table 1 shows upper limits in relative difference between the closed form solution and the numerical 2-dimensional solution.

Table 1. Limits to relative difference between 1-dim and 2-dim solutions for $0.5 < \varepsilon < 0.95$

		κ								
		0.01	0.02	0.05	0.1	0.2	0.5	1	2	5
L/d	0.1	0.9	0.9	0.9	0.95	0.95	0.95	0.95	0.95	0.95
	0.3	0.7	0.7	0.7	0.7	0.75	0.8	0.9	0.9	0.9
	0.5						0.7	0.8	0.85	0.9

The table should be read like this: At for example $L/d = 0.1$ and $\kappa = 1$, the 2-dim solution is within 0.95 of the 1-dim solution.

OPTIMIZING

Minimum film thickness puts an upper limit to eccentricity. At small eccentricities the load capacity will be insufficient. A suitable choice is:

$$0.7 < \varepsilon < 0.95$$

Within this range we want the load capacity to be as large as possible and friction low. This is achieved if:

$$0.1 < \kappa < 0.5$$

A large length of L a conical section gives high load capacity and low friction, but may interfere with other purposes, such as a need for several cylindrical sections and balancing of forces. Side flow will increase with L. A reasonable limit is

$$L/d < 1$$

We have now established limits to ε , κ and L/d .

OIL CONSUMPTION, TEMPERATURE RISE AND FRICTION

The oil consumption can be estimated with the method outlined in (4) or standard engineering formulas. The temperature rise is negligible in most cases since the slider speed is low and the bearing surface large. The friction can be calculated in the same way as the load capacity utilizing pad bearing theory.

Friction

For a pad bearing of infinite width the friction force per unit width is (3):

$$F_{\text{fric}} := \eta \cdot v \cdot \frac{L}{h_0} \cdot \frac{1}{k} \cdot \left(4 \cdot \ln(1+k) - \frac{6 \cdot k}{2+k} \right)$$

The friction force then becomes

$$F_{\text{fric}} := \eta \cdot v \cdot \frac{L}{\psi \cdot d} \cdot \frac{2}{\kappa} \cdot \left(4 \cdot \ln(1+k) - \frac{6 \cdot k}{2+k} \right) \cdot \frac{d}{2} \cdot d\theta$$

Summing around the circumference

$$W_{\text{fric}} := \eta \cdot v \cdot \frac{L}{\psi} \cdot \int_0^\pi \frac{2}{\kappa} \cdot \left(4 \cdot \ln(1+k) - \frac{6 \cdot k}{2+k} \right) d\theta$$

It is now possible to formulate a friction number

$$\mu := \frac{W_{\text{fric}}}{W}$$

Where, as before

$$W := \eta \cdot v \cdot d \cdot \left(\frac{L}{\psi \cdot d} \right)^2 \cdot W_0(\varepsilon, \kappa)$$

After abbreviations this becomes

$$\mu(\varepsilon, \kappa) := \frac{\psi \cdot d}{L} \cdot \frac{W_{\text{fric}0}}{W_0}$$

Where

$$W_{\text{fric}0} := \int_0^\pi \frac{2}{\kappa} \cdot \left(4 \cdot \ln(1+k) - \frac{6 \cdot k}{2+k} \right) d\theta$$

The friction number can be written as a product of case specifics and a dimensionless function

$$\mu(\varepsilon, \kappa) := \frac{\psi \cdot d}{L} \cdot \mu_0(\varepsilon, \kappa)$$

The general friction number μ_0 is easily calculated, figure 14.

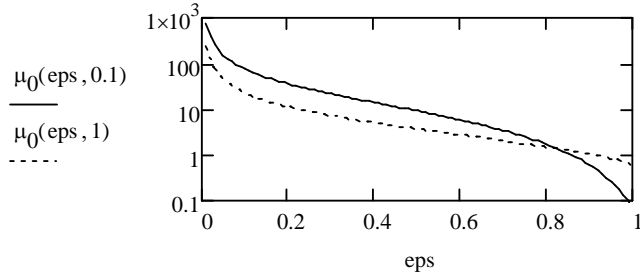


Figure 14. Friction number μ_0 as a function of eccentricity ε , for $\kappa = 0.1$ and $\kappa = 1$

To get a feel for the friction number, let us assume that $\psi = 0.003$, and that $d/L = 3$. Then the coefficient of friction is shown in figure 15.

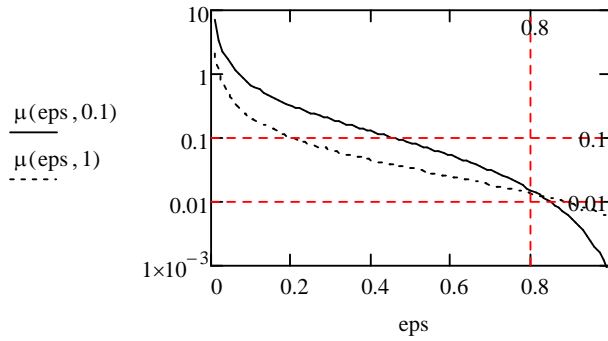


Figure 15. Friction number for $\psi = 0.003$ and $d/L = 3$ as a function of eccentricity ε and κ

And finally, by plotting friction number μ_0 as a function of kappa for different eccentricities we see that minimum friction is achieved for $0.1 < \kappa < 1$

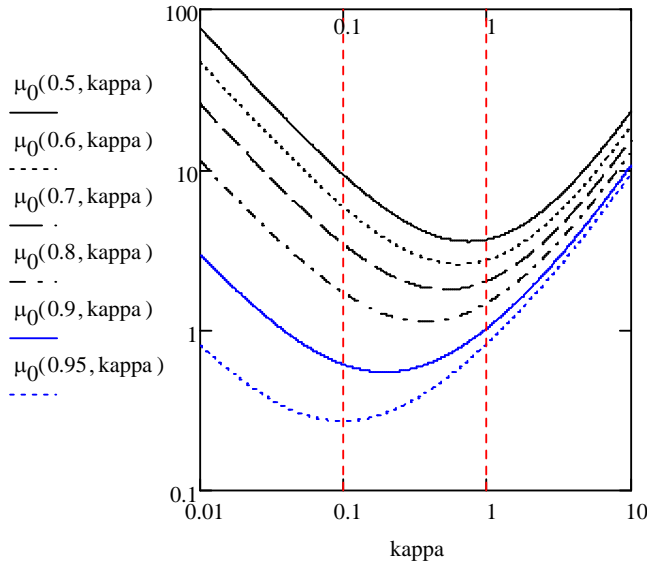


Figure 16. Minimum friction is achieved for $0.1 < \kappa < 1$

THE INFLUENCE OF OIL GROOVES

In order to supply the bearing with oil, grooves are machined in the bushing. When the load acts in one plane only it is good practice to have two oil grooves, one on each side of the load plane, opposed to each other, as in fig 18. In this case the influence on the load capacity due to zero pressure at the oil grooves is practically negligible when the length of the profiled section is equal to or less than the slider diameter as can be seen in diagrams 19 and 20.

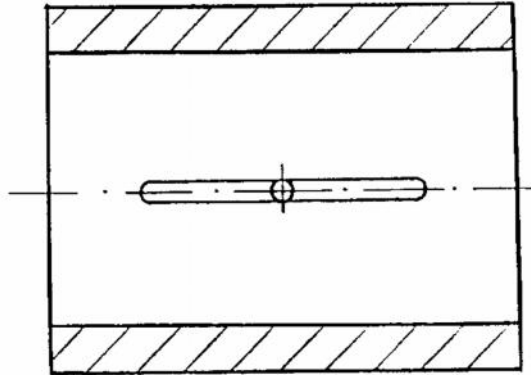


Figure 17. Bushing with oil groove

In this case the influence on the load capacity due to zero pressure at the oil grooves is practically negligible when the length of the profiled section is equal to or less than the slider diameter as can be seen in diagrams 19 and 20.

DESIGN RULES

From the above, general fluid film bearing theory and practical application the following design rules have been found to apply:

a/ the relative clearance ψ should be as small as machining and/or thermal expansion permits

b/ the profiled sections should be long, but considerably shorter than the slider diameter.

$$3 < d/L < 10$$

c/ the smallest film thickness h_0 should be greater than 3-5 Ra of the mating surfaces. This gives an upper limit to ε :

$$\max \varepsilon = 1-2 h_0 / (\psi d)$$

d/ the profile parameter κ must be less than one. Optimum:

$$0.1 < \kappa < 0.5$$

e/ a suitable relation between the length L of the profiled section and the length cL of the cylindrical section of the slider is in the range:

$$0.2 < c < 0.5$$

REFERENCES

- (1) Ingalls, A.G.: Ruling Engines, Scientific American, June, 1952, p 45-54.
- (2) Seybold, R.: Geradföhrungen mit dynamischer Schmierung - ein Beitrag zur Gestaltung und Auslegung von Geradföhrungen, Konstruktion 31 (1979) h.10, p 319-403.
- (3) Jakobsson, B. and Floberg L.: The rectangular Plane Pad Bearing, Transactions of Chalmers university of technology, Gothenburg, Sweden, no 203, 1958.
- (4) Brendel, H.: Wissensspeicher Tribotechnik, Springer-Verlag, 1978, p 147-163.
- (5) Brendel, H.: Die Tragfähigkeit einer hydrodynamisch gestalten zylindrischen Langsföhrung bei statischen Laufbedingungen. Wiss. Zeitschrift der TH Karl-Marx Stadt, Jg III (1970) H. 1.
- (6) Brendel, H.: Berechnung einer hydrodynamischen Zylindrischen Föhrung mit Hilfe eines Nomogramms, Schmierungstechnik 4 (1973) 9, p 259-264.
- (7) Brendel, H. and Lam Quanghai: Zur tribotechnischen Föhrungen. Wiss. Zeitschrift der TH Karl-Marx-Stadt. Jg XIX, 1977, Heft 1.
- (8) Brendel, H and Lam Quanghai: Die Reibkraft an Profilierten zylindrischen Föhrungen mit Flüssigkeitsreibung (PZF-Föhrung), Wissenschaftliche Zeitschrift der Technische Hochschule Karl-Marx-Stadt (1978), Heft 1, p 3-15.

